LA-UR-14-29153 (Accepted Manuscript)

The occurrence of non-pulsating stars in the Dor and Sct pulsation instability regions: results from quarter 14–17 data

Guzik, Joyce Ann
Bradley, Paul Andrew
Jackiewicz, Jason
Molenda-Zakowicz, Joanna
Uytterhoeven, Katrien
Kinemuchi, Karen

To be published in: Astronomical Review

DOI to publisher's version: 10.1080/21672857.2015.1023120

Permalink to record: http://permalink.lanl.gov/object/view?what=info:lanl-repo/lareport/LA-UR-14-29153

Astronomical Review

ISSN: 2167-2857 (Print) 2167-2865 (Online) Journal homepage: http://www.tandfonline.com/loi/tare20

The occurrence of non-pulsating stars in the γ Dor and δ Sct pulsation instability regions: results from Kepler quarter 14–17 data

J.A. Guzik, P.A. Bradley, J. Jackiewicz, J. Molenda-Zakowicz, K. Uytterhoeven & K. Kinemuchi

To cite this article: J.A. Guzik, P.A. Bradley, J. Jackiewicz, J. Molenda-Zakowicz, K. Uytterhoeven & K. Kinemuchi (2015) The occurrence of non-pulsating stars in the γ Dor and δ Sct pulsation instability regions: results from Kepler quarter 14–17 data, Astronomical Review, 11:1, 1-24, DOI: 10.1080/21672857.2015.1023120

To link to this article: http://dx.doi.org/10.1080/21672857.2015.1023120

Accepted author version posted online: 25 Mar 2015.
Published online: 21 Apr 2015.

Astronomical Review, 2015
Vol. 11, No. 1, 1–24, http://dx.doi.org/10.1080/21672857.2015.1023120

Taylor & Francis
Taylor & Francis Group

The occurrence of non-pulsating stars in the γ Dor and δ Sct pulsation instability regions: results from *Kepler* quarter 14–17 data

J.A. Guzik[a]*, P.A. Bradley[b], J. Jackiewicz[c], J. Molenda-Zakowicz[c,d], K. Uytterhoeven[e,f] and K. Kinemuchi[g]

[a]*X-Theoretical Design Division, Los Alamos National Laboratory, Los Alamos, NM, USA;* [b]*X-Computational Physics Division, Los Alamos National Laboratory, Los Alamos, NM, USA;* [c]*Department of Astronomy, New Mexico State University, Las Cruces, NM, USA;* [d]*Instytut Astronomiczny, Uniwersytet Wroclawski, Wroclaw, Poland;* [e]*Instituto de Astrofisica de Canarias (IAC), La Laguna, Spain;* [f]*Dept. Astrofisica, Universidad de La Laguna, La Laguna, Spain;* [g]*Apache Point Observatory, Sunspot, NM, USA*

The high precision long time-series photometry of the NASA *Kepler* spacecraft provides an excellent means to discover and characterize variability in main-sequence stars, and to make progress in interpreting the pulsations to derive stellar interior structure and test stellar models. For stars of spectral types A–F, the *Kepler* data revealed a number of surprises, such as more hybrid pulsating δ Sct and γ Dor pulsators than expected, pulsators lying outside of the instability regions predicted by theory, and stars that were expected to pulsate, but showed no variability. In our 2013 *Astronomical Review* article, we discussed the statistics of variability for 633 faint (*Kepler* magnitude 14–16) spectral type A–F stars observed by *Kepler* during Quarters 6–13 (June 2010–June 2012). We found six stars that showed no variability with amplitude 20 ppm or greater in the range 0.2–24.4 cycles/day, but whose positions in the $\log g - T_{\rm eff}$ diagram place them in the δ Sct or γ Dor pulsation instability regions established from pre-*Kepler* ground-based observations. Here, we present results for an additional 2137 stars observed during Quarters 14–17 (June 2012–May 2013). This sample is not unbiased, as we limited our target list to stars showing variability in Quarter 0 full-frame images to enhance our variable star discovery rate. We find that 990 stars, or 46%, show no frequencies in the Fourier transform of their light curves down to the 20-ppm level, a smaller percentage than the 60% of our Q6–13 sample. We find 34 additional stars that lie within the ground-based γ Dor/δ Sct pulsation instability regions; their lack of pulsations requires explanation. In the analysis for our first paper, we included a +229 K offset to the *Kepler* Input Catalog $T_{\rm eff}$ to take into account an average systematic difference between the KIC values and the $T_{\rm eff}$ derived from SDSS color photometry for main-sequence F stars. We compare the KIC $T_{\rm eff}$ value and the $T_{\rm eff}$ derived from spectroscopy taken by the LAMOST instrument for 54 stars common to both samples. We find no trend to support applying this offset; the trend instead shows that a small average temperature *decrease* relative to the KIC $T_{\rm eff}$ may be more appropriate for the stars in our spectral-type range. If the 229 K offset is omitted, only 17 of our 34 "constant" stars fall within the pulsation instability regions. The comparisons with LAMOST-derived $\log g$ also show that the KIC $\log g$ may be too large for stars with KIC $\log g$ values >4.2. For the two "constant" stars in the instability region that were also observed by LAMOST, the LAMOST $T_{\rm eff}$ values are cooler than the KIC $T_{\rm eff}$ by several hundred K, and would move these stars out of the instability regions. It is possible that a more accurate determination of their $T_{\rm eff}$ and $\log g$ would move some of the other

*Corresponding author. Email: joy@lanl.gov

"constant" stars outside of the instability regions. However, if average (random) errors in $T_{\rm eff}$ ($\pm$290 K) and an offset in log g from the KIC values are taken into account, 15–52 stars still persist within the instability regions. Explanations for these "constant" stars, both theoretical and observational, remain to be investigated.

Keywords: stars; pulsations – stars; oscillations – stars; δ Scuti – stars; γ Doradus

1. Introduction

The NASA *Kepler* spacecraft was launched 7 March 2009 with the mission to detect transits of Earth-sized planets around sun-like stars using high precision CCD photometry.[1] As a secondary mission, *Kepler* photometry has also been used to survey many thousands of stars for variability and stellar activity.[2]

Through the NASA *Kepler* Guest Observer program Cycles 1–4, we requested and received observations of 2770 stars of spectral types A–F. Our goals are to search for pulsating γ Dor and δ Sct variable star candidates, identify "hybrid" stars pulsating in both types that are especially useful for asteroseismology and testing stellar pulsation theory, characterize the frequency content, and look for amplitude variability. In the course of these observations, we discovered many eclipsing binary stars, stars that are probably not pulsating but show low-frequency photometric variations due to stellar activity or rotating star spots, and many stars that show no variability at the frequencies

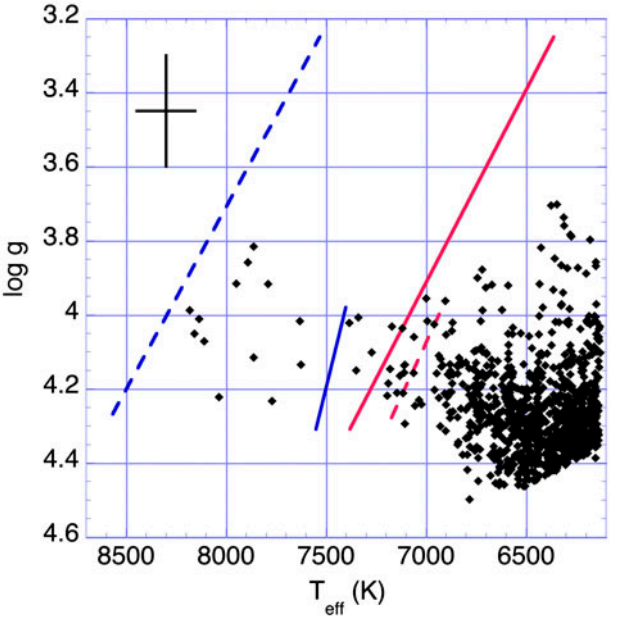

Figure 1a. Location of sample stars that are "constant" (see definition in text) in the log surface gravity – $T_{\rm eff}$ diagram, along with δ Sct (dashed lines) and γ Dor (solid lines) instability strip boundaries established from pre-*Kepler* ground-based observations.[26,27] The $T_{\rm eff}$ of the sample stars has been shifted by +229 K to account for the systematic offset between $T_{\rm eff}$ of the *Kepler* Input Catalog and SDSS photometry for this temperature range as determined by [28]. The black cross shows an error bar on log g (0.3 dex) and $T_{\rm eff}$ (290 K) established by comparisons of KIC values and values derived from ground-based spectroscopy for brighter *Kepler* targets.[19]

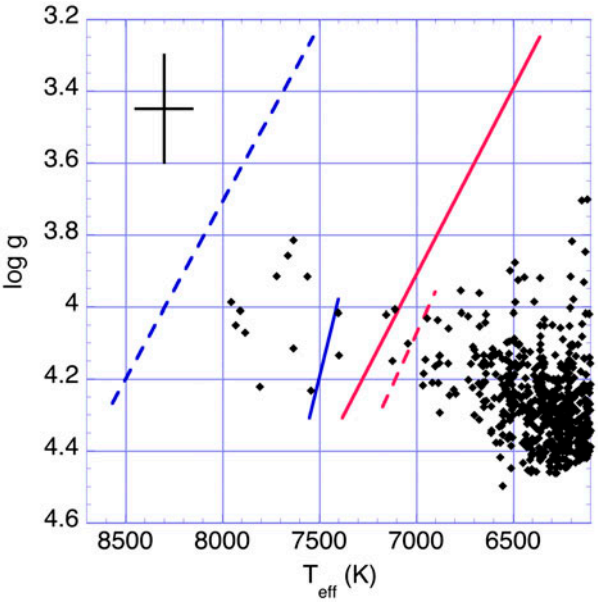

Figure 1b. Same as Figure 1a, but without the +229 K offset applied to the KIC $T_{\rm eff}$ values. Without the offset, only 17 stars lie within the pulsation instability regions.

expected for γ Dor or δ Sct stars. An initial identification and categorization of the pulsating, binary, and spotted star candidates is given by [3,4]. A search for pulsations in one or more components of the eclipsing binaries in this sample has been started by [5].

Paper 1 [6] (see also [7]) discussed the number of "constant" stars, defined as having no frequencies with amplitude above 20 ppm in the frequency range of 0.2–24.4 cycles/day in long-cadence data on an unbiased sample of 633 stars observed during Quarters 6–13. We found that about 60% of the stars were "constant" by this definition. We also identified six possible "constant" stars that lie within the boundaries of the δ Sct or γ Dor pulsation instability regions as established by pre-*Kepler* ground-based observations. This paper considers the "constant" stars in the larger not-unbiased sample of 2137 stars observed in long cadence during Q14–17, until the *Kepler* observations in the Cygnus–Lyra region ended after the failure of the spacecraft's second reaction wheel.

2. Description of γ Dor and δ Sct pulsators

The γ Doradus stars are late-A to F-type main sequence variables showing multiple periods of 0.3–3 days that have been identified as high-order, low-degree non-radial gravity (g) modes. The intrinsic variability of the prototype γ Doradus was discussed by [8], and the new class with 15 members was described by [9]. Since then, over 60 members of the class have been identified [10] using ground-based observations.[11] proposed "convective blocking" at the base of the envelope convective zones as the driving mechanism for γ Dor g modes. When the temperature at the convective envelope base is between 200,000 and 500,000 K, the convective timescale

Table 1. KIC number, effective temperature, log g, and *Kepler* magnitude for 34 "constant" stars that lie within the pre-*Kepler* pulsation instability regions.

KIC number	KIC $T_{\rm eff}$ (K)	KIC $T_{\rm eff}$ + 229 K	KIC log g	$K_{\rm p}$ mag
4465403	7954	8183	3.988	14.498
5630494	7931	8160	4.051	14.078
7685485	7907	8136	4.011	14.339
5952417	7882	8111	4.071	15.064
8246744	7807	8036	4.222	14.622
8707758	7720	7949	3.916	14.091
7620739	7663	7892	3.858	14.621
6139295	7634	7863	4.115	14.374
7467076	7634	7863	3.816	14.67
4661844	7562	7791	3.917	14.921
6279284	7543	7772	4.233	14.661
7595223	7402	7631	4.017	14.442
9590213	7398	7627	4.135	14.432
8580178	7155	7384	4.022	14.597
5096805	7122	7351	4.15	14.51
4171238	7110	7339	4.007	14.227
3729981	7043	7272	4.101	14.084
9016039	6966	7195	4.218	14.267
8355866	6961	7190	4.185	14.349
7751249	6952	7181	4.146	14.066
7668077	6943	7172	4.031	14.34
6522027	6916	7145	4.21	14.291
6696719	6902	7131	4.165	14.274
7517640	6890	7119	4.036	14.767
6530559	6886	7115	4.211	14.912
6124552	6880	7109	4.156	14.33
8292900	6880	7109	4.136	14.307
7364349	6878	7107	4.135	14.421
5950897	6835	7064	4.157	14.401
6035807	6833	7062	4.06	15.413
5089044	6771	7000	3.956	14.594
4375039	6766	6995	4.017	14.558
3444020	6732	6961	4.026	14.727
4271591	6675	6904	3.962	15.00

(mixing length/convective velocity) at this location is comparable to or longer than the g-mode pulsation period. Since convection takes a portion of the pulsation cycle to turn on and transport the emergent luminosity, luminosity is periodically blocked, resulting in pulsation driving. This mechanism predicts unstable g modes in exactly the observed period range, and has become the accepted mechanism for γ Dor pulsation driving (see also [12–14]).

The δ Scuti stars, on the other hand, pulsate in low-order radial and non-radial pressure (p) modes, although some of their modes have mixed p- and g-mode character; about 630 were catalogued as of 2000.[15] Their instability strip lies on the main sequence between early A and early F spectral types, and their periods range from just under 30 min to about 0.3 days. Their pulsations are driven by the second ionization of helium that locally increases the opacity and regulates radiation flow in the envelope layers at $\sim$50,000 K (the "κ effect"; see e.g. [16]).

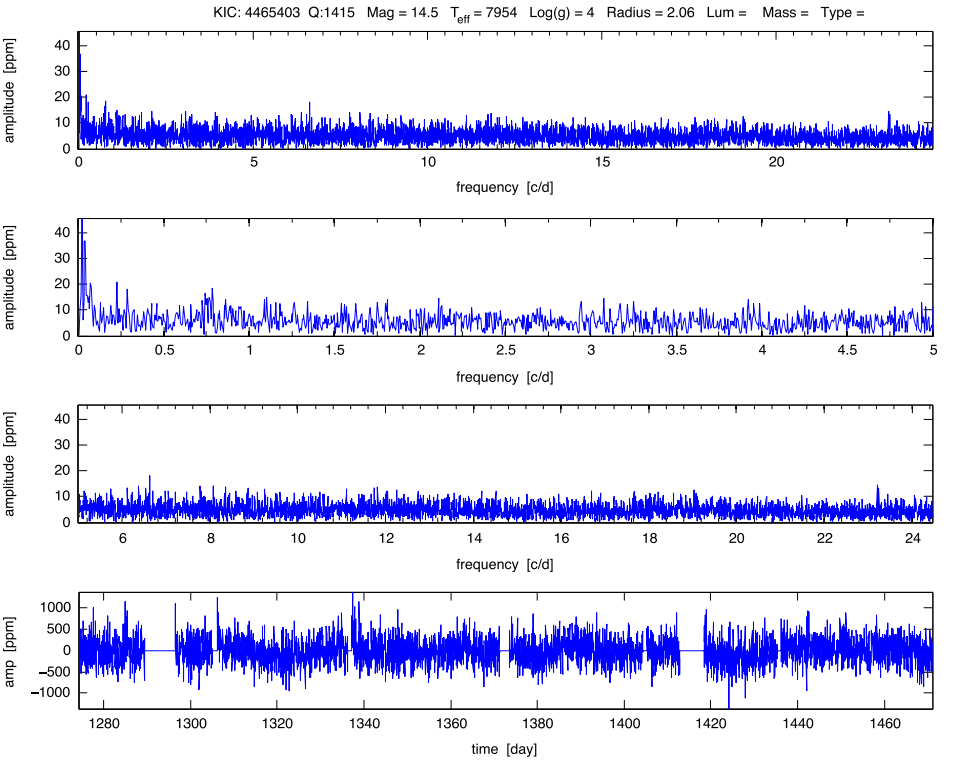

Figure 2a. Amplitude spectrum (top 3 panels) and light curve (bottom panel) for KIC 4465403, the hottest of the "constant" stars within the δ Sct instability strip boundary in Figures 1a and 1b. The noise level for this faint star is at about the 10 ppm level.

The γ Dor and δ Sct stars are interesting asteroseismically because they form a bridge between the lower mass solar-like stars with large convective envelopes and slow rotation, and the more massive, rapidly rotating stars with convective cores. The δ Sct and γ Dor stars have both convective cores and convective envelopes, a variety of rotation rates, and live long enough for element settling, diffusion, and radiative levitation to alter their surface abundances and cause chemical peculiarities. The envelope convection zones of the hotter and more massive δ Sct stars are confined to smaller regions (around 10,000–50,000 K) where hydrogen and helium are ionizing, and where convection transports a small fraction of the luminosity. The envelope convection zones become deeper and carry a larger fraction of the star's luminosity with increasing stellar age and/or decreasing stellar mass (see e.g. [17] and references therein). Both γ Dor and δ Sct stars pulsate in multiple modes that probe both the core and envelope. The pulsations of these stars can be used to diagnose these phenomena and test stellar models.

Hybrid γ Dor/δ Sct stars are among the most interesting targets for asteroseismology because the two types of modes (pressure and gravity) probe different regions of the star and are sensitive to the details of the two different driving mechanisms. Because these driving mechanisms are somewhat mutually exclusive, hybrid stars exhibiting both types of pulsations are expected theoretically to exist only in a small

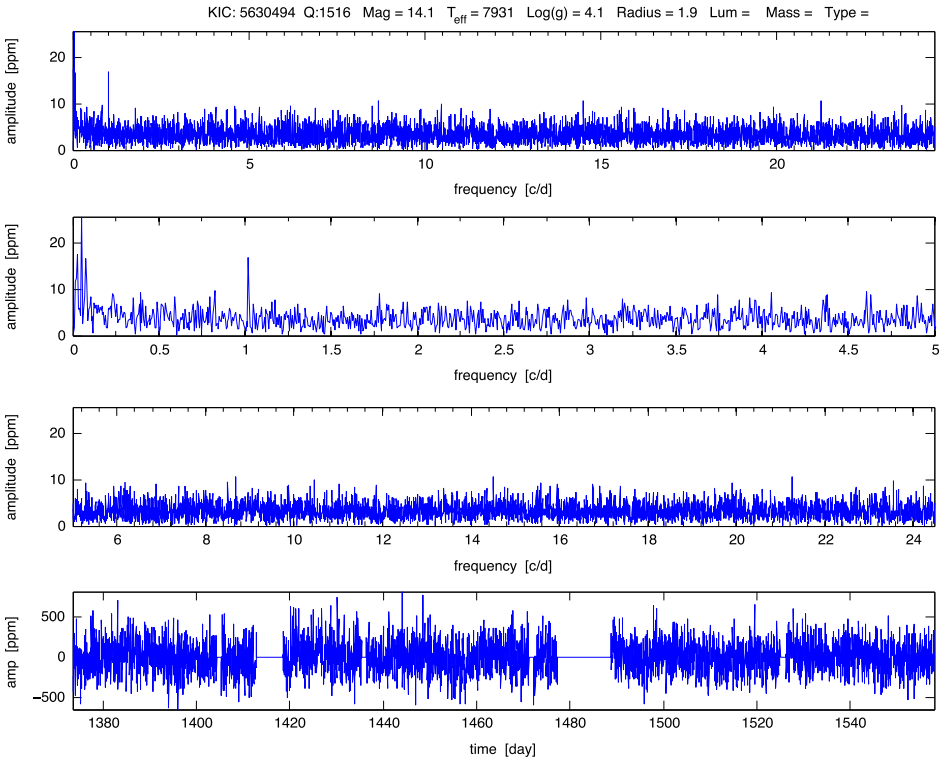

Figure 2b. Amplitude spectrum (top 3 panels) and light curve (bottom panel) for KIC 5630494, another hot "constant" star within the δ Sct instability region in Figures 1a and 1b. The noise level is about 7 ppm. One probably non-significant frequency at about 1 c/d is evident with amplitude about 17 ppm.

overlapping region of temperature-luminosity space in the Hertzsprung–Russell (H–R) diagram.[12,13]

Before the advent of the *Kepler* and CoRoT space missions, only four hybrid γ Dor/δ Sct pulsators had been discovered. However, the first published analysis by the *Kepler* Asteroseismic Science Consortium (KASC) of 234 targets showing pulsations of either type revealed hybrid behavior in essentially all of them.[18] In a study of 750 KASC A–F stars observed for four quarters,[19] 475 stars showed either δ Sct or γ Dor variability, and 36% of these were hybrids. The *Kepler* hybrids were not confined to a small overlapping region of the two instability types in the temperature-luminosity space of the H–R diagram as predicted by theory. Instead, they are found in the $T_{\rm eff}$–log g diagram throughout both the predicted γ Dor and δ Sct instability regions, and even at cooler and hotter temperatures outside these regions. Despite extensive study of this large sample and of the public data,[20] no obvious frequency or amplitude correlations with stellar properties have emerged, and there seems to be no clear observed separation of γ Dor and δ Sct pulsators in the H–R diagram. The known driving mechanisms cannot explain the pulsation behavior.

The existence and properties of these *Kepler* variable star candidates raise a number of questions: Why are hybrids much more common than predicted by theory? Are additional pulsation driving mechanisms at work? Why are there apparently "constant" stars

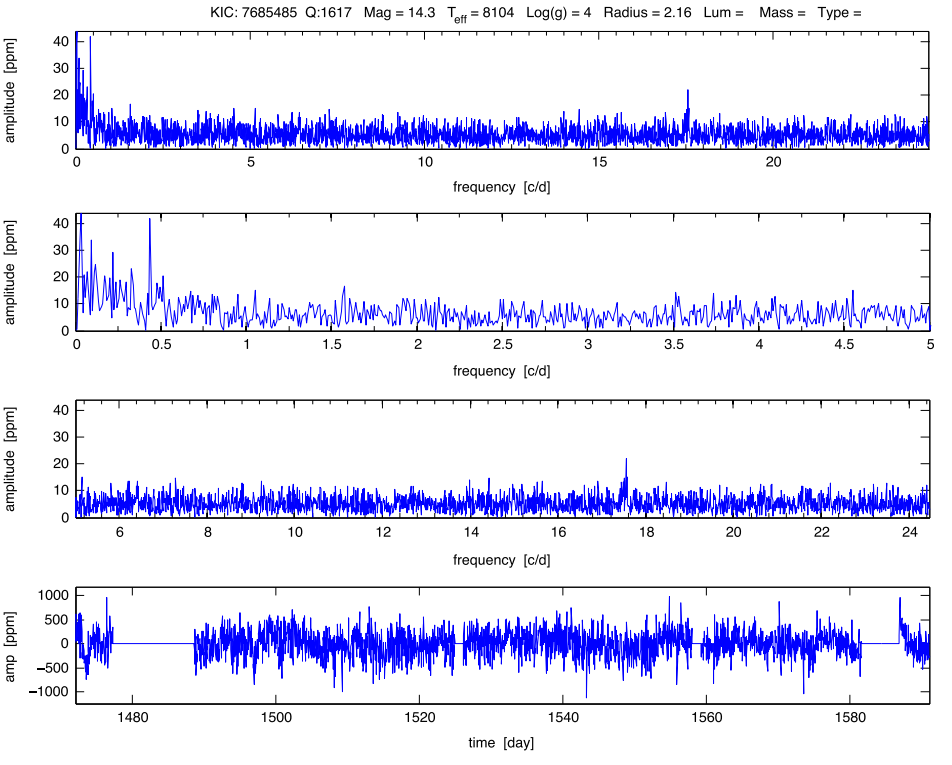

Figure 2c. Amplitude spectrum (top 3 panels) and light curve (bottom panel) for KIC 7685485, another hot "constant" star within the δ Sct instability region in Figures 1a and 1b. The noise level is about 10 ppm. One frequency at about 0.4 c/d with amplitude of 40 ppm is evident, but a longer data-set is needed to confirm. The frequency at about 17.5 c/d is present for many of the stars in the Q16–Q17 data-sets and is an artifact.

that lie within the instability regions but show no pulsation frequencies in the γ Dor or δ Sct frequency range?

3. Target selection and data processing

We examined the *Kepler* data on the 2137 stars observed for *Kepler* Guest Observer Cycle 4 during Quarters 14–17 spanning the period from 28 June 2012 to 8 May 2013. These stars are relatively faint, with *Kepler* magnitudes 14–16. We requested only long-cadence data, with integration time per data point of 29.4 min.[21] The Fourier transform of this data will be able to detect frequencies less than the Nyquist frequency, or half the sampling frequency, which is 24.4 cycles/day. However, because γ Dor stars have frequencies of about 1 cycle/day, and most δ Sct stars have frequencies of 10–20 cycles/day, the long-cadence data are adequate to identify γ Dor and most δ Sct candidates. Also, as discussed below, super-Nyquist frequencies will appear mirrored at sub-Nyquist frequencies [22] and therefore will be detected in the amplitude spectrum, if they exist.

We chose these stars by using the *Kepler* Guest Observer target selection tool to search the *Kepler* Input Catalog [23, KIC]. For Q6–13 discussed in Paper 1, we

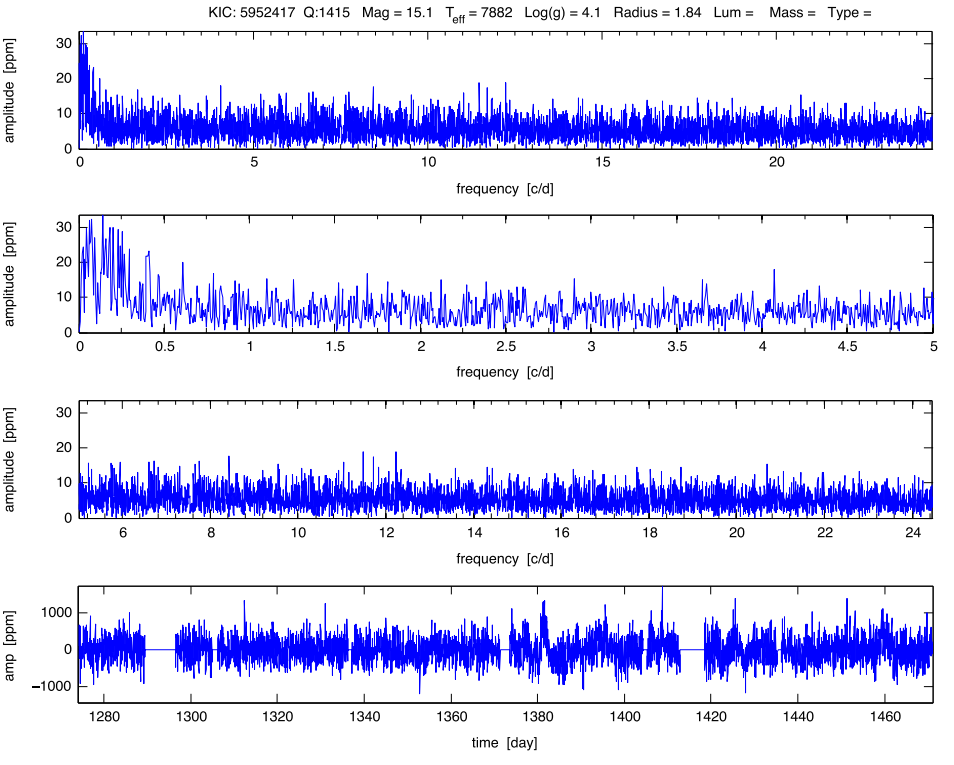

Figure 2d. Amplitude spectrum (top 3 panels) and light curve (bottom panel) for KIC 5952417, another hot "constant" star within the δ Sct instability region in Figures 1a and 1b. The noise level is about 10 ppm.

restricted our sample to stars in or near the γ Dor/δ Sct instability regions, with effective temperature $6200 < T_{\rm eff} < 8300$ K; surface gravity $3.6 < \log g < 4.7$, contamination or blend from background stars 0.01, and *Kepler* Flag 0, meaning that these targets had not yet been observed by *Kepler*. Most of the brighter stars had already been observed by either the *Kepler* Science Team, or KASC, and these are discussed by [19]. For Quarter 14–17 targets observed for our Cycle 4 Guest Observer proposal reported here, the selection was not unbiased, but instead was cross-correlated with a list of potentially variable stars identified by comparing full-frame images taken during the *Kepler* spacecraft commissioning period.[24] In our target search, we shifted our criteria to lower temperatures (5900–8000 K), as we were finding many stars with γ Dor and δ Sct pulsations at lower $T_{\rm eff}$. We also relaxed the contamination factor criteria to 0.05. This search yielded a sample of over 6000 stars that we cross-correlated against the $\sim$300,000 stars in the *Kepler* field found to be variable by [24] by comparing the Q0 full-frame images. The cross-correlation returned 2174 stars, of which we received data for 2137 stars.

After downloading the data files from the MAST (Mikulski Archive for Space Telescopes, http://archive.stsci.edu/index.html), we processed them using Matlab scripts developed by J. Jackiewicz. We combined data for all available quarters for each star. We chose to use the data corrected by the *Kepler* pipeline; we have also tried using the

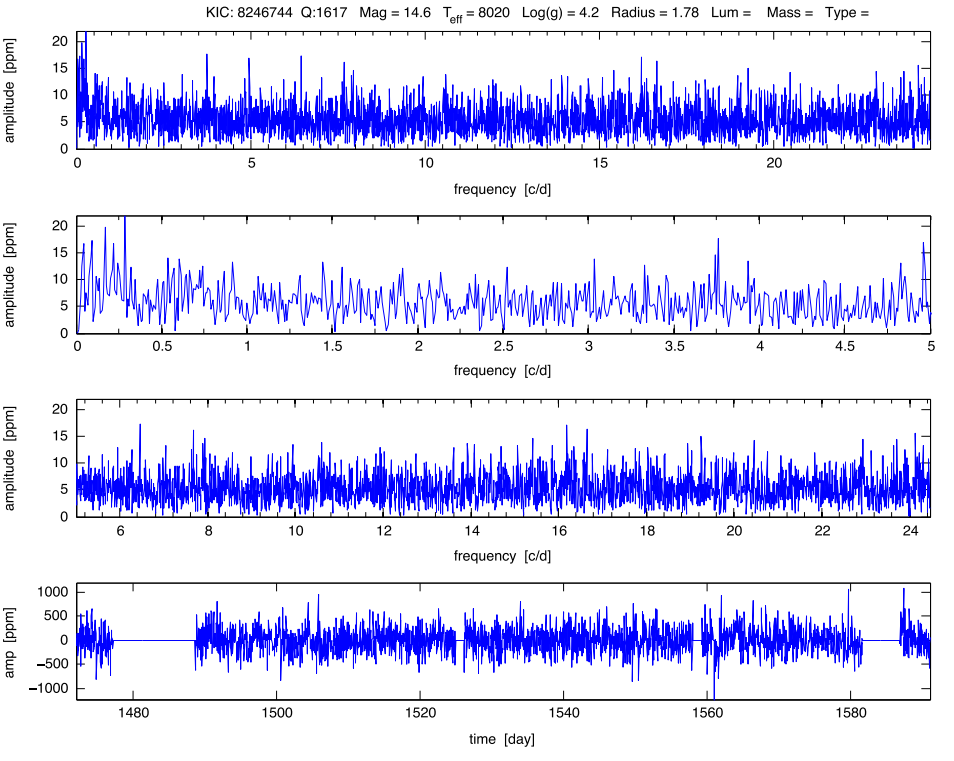

Figure 2e. Amplitude spectrum (top 3 panels) and light curve (bottom panel) for KIC 8246744, another hot "constant" star within the δ Sct instability region in Figures 1a and 1b. The noise level is about 10 ppm.

raw light curves, and found essentially no difference in the frequencies found by the Fourier transform.

The Matlab scripts remove outlier points and interpolate the light curves to an equidistant time grid. The light curves are then converted from *Kepler* flux (F_K) to parts per million (ppm) using the formula $f(t) = 10^6(F_K/y - 1)$, where y is either the mean value of the entire light curve, or a low-order polynomial fit to the light curve, depending on artifacts present in the data (see also [25]). After the processing and Fourier transform of the data, the Matlab scripts generate a plot for each star, such as the examples shown in Figures 2a–2f. In these plots, the bottom panel is the light curve in ppm vs. time; the top panel shows the amplitude in ppm vs. frequency in cycles/day determined by the Fourier transform, and the middle two panels are enlargements of the frequency ranges 0–5 cycles/day and 5–24.4 cycles/day. The header on each panel shows the KIC number, the Quarters of observation, the *Kepler* magnitude, and log surface gravity (log g, rounded to two digits). The radius in the header is also from the KIC but is not accurate, as it is derived by assuming a stellar mass of 1 $M_\odot$ and using the log surface gravity (log g) of the KIC.

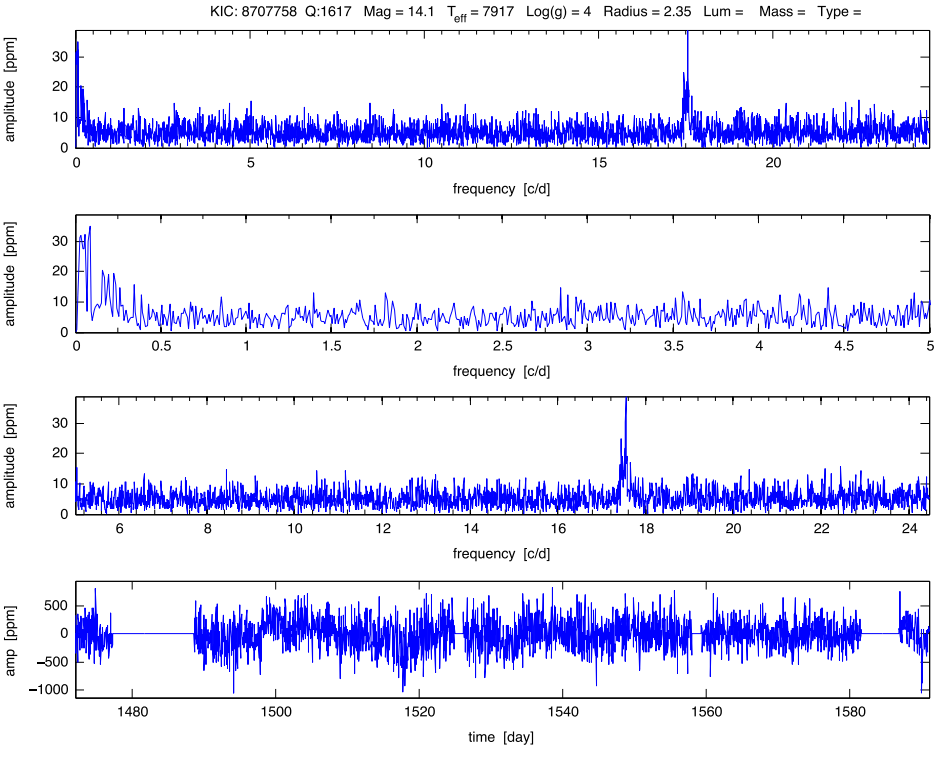

Figure 2f. Amplitude spectrum (top 3 panels) and light curve (bottom panel) for KIC 8707758, another hot "constant" star within the δ Sct instability region in Figures 1a and 1b. The noise level is about 10 ppm; the artifact frequency $\sim$17.5 c/d also evident in Figure 2b is clearly seen.

4. Identification and distribution of "constant" stars in the H–R diagram

As in Paper 1, we examined individually the Matlab-generated plots for our sample of 2137 stars. We flagged as "constant" the stars with no power in the spectrum from 0.2 to 24.4 c/d above 20 ppm.

There is some judgment involved in deciding whether a given star meets these criteria. For some stars, the noise level over a good portion of this frequency range is about 20 ppm. For many stars, stellar activity may cause photometric variations and power in the spectrum at slightly above the 20 ppm level at 0.2–0.5 c/d frequencies. We eliminated from consideration stars that appear to be eclipsing binaries that may have stellar components that individually turn out to be either "constant" or variable once the binary signal is removed. We have begun analysis of the binaries.[5]

In Paper 1, by these criteria we found 359 "constant" stars out of the 633 stars in our sample, or roughly 60%. Here, with this preconditioned sample, we found 990 out of 2137 stars, or 46% that are "constant". We plotted the position of the "constant" stars in a log surface gravity vs. $T_{\rm eff}$ diagram (1a), along with the δ Sct (dashed lines) and γ Dor (solid lines) instability strip boundaries established from pre-*Kepler* ground-based observations.[26,27] We show with a black cross the error bar on log g (0.3 dex) and $T_{\rm eff}$ (290 K) derived by comparing KIC values of brighter *Kepler* targets with those derived from ground-based spectroscopy, as discussed by [19].

Table 2. Spectral type, $T_{\rm eff}$, and log g determined from LAMOST spectra for 54 stars in common with our sample.

KIC number	$K_{\rm p}$ mag	LAMOST spectral type	KIC $T_{\rm eff}$	LAMOST $T_{\rm eff}$	LAMOST $T_{\rm eff}$ error	KIC log g[c]	LAMOST log g	LAMOST log g error
4374006	14.407	F5V	6071	5851	137	4.399	4.22	0.14
4561941	14.552	F2V	6348	6268	213	3.772	4.13	0.12
4568087	14.781	F0IV	7153	6898	121	4.127	4.1	0.11
4735997	14.716	F4V	6048	6085	211	4.135	4.19	0.11
4929320	14.496	G0V	5914	5856	121	4.318	4.14	0.21
4995588	14.961	A5IV	7401	7700	156	4.16	3.86	0.14
4999718	14.444	F5	6331	6202	98	4.405	4.19	0.12
5088361	15.109	F5	6299	6050	129	4.289	4.2	0.11
5096460	14.135	F5V	6826	6569	132	4.1	4.14	0.11
5096805[b]	14.510	F4V	7122	6541	128	4.15	4.13	0.12
5168478	14.473	F3/F5V	6211	6397	81	4.174	4.17	0.1
5257286	14.326	F5V	6429	5855	84	4.483	4.17	0.11
5342935	14.033	F5V	6558	6595	128	4.36	4.14	0.11
5437797	14.370	F8V	5971	5738	71	4.26	4.2	0.15
5610296	14.846	F5	6348	6078	128	4.429	4.21	0.12
5629082	14.026	G0V	5967	5929	120	4.283	4.15	0.13
5629366[a]	14.002	G0V	6012	5904	141	3.873	4.11	0.17
5629366	14.002	G0V	6012	5928	118	3.873	4.12	0.16
5685860	14.385	F5	6022	6120	131	4.271	4.21	0.12
5716288	14.301	F6IV	6398	6367	142	4.453	4.09	0.15
5783368	14.806	A6V	7910	7958	107	3.835	3.96	0.11
5809732	14.098	F1V	6613	6891	156	4.122	4.09	0.11
5858178	14.416	F5	6088	5971	136	4.325	4.19	0.12
6113533	14.409	F8V	6081	6019	106	4.355	4.13	0.13
6132246	14.462	F4V	6539	6504	89	4.227	4.12	0.11
6207546	14.321	F5V	7134	6569	142	4.305	4.14	0.11
6292725	14.168	F7III	5905	5776	184	4.141	4.14	0.26
6446706	14.826	F6V	6217	6393	167	4.329	4.12	0.13
6446775	14.348	G0V	6133	6004	110	4.383	4.19	0.13
6452044	14.218	F2V	6510	6386	82	4.23	4.13	0.12
6526666	14.176	F0V	6832	6504	99	4.219	4.12	0.11
6696719[b]	14.274	F3V	6902	6507	84	4.165	4.13	0.11
7038888	14.316	F0V	6812	6647	106	4.198	4.14	0.11
7191541	14.303	F7IV	6633	6317	98	4.25	4.1	0.13
7205852	14.393	F5	6253	6250	105	4.352	4.13	0.12
7439291	14.329	F5	6380	6204	90	4.212	4.15	0.12
7448387	14.716	G5V	6315	5817	110	4.199	4.11	0.18
7729149	14.024	F5V	6442	6394	74	4.273	4.11	0.11
7746728	14.446	F8V	6081	6077	115	4.379	4.08	0.13
7748881	14.143	F6V	6367	6242	131	4.262	4.19	0.11
8082314	14.299	G5	5917	5819	95	4.206	4.24	0.14
8158284	14.415	G5	5995	5858	89	4.36	4.19	0.14
8316032	14.511	F3V	6250	6467	108	3.979	4.14	0.11
8327183	14.080	F7IV	6021	6333	109	4.198	4.13	0.12
8361689	14.647	F8V	6201	6215	75	4.42	4.13	0.13
8414160	14.193	G0V	6491	6221	95	4.228	4.14	0.12
8415383	14.010	F1V	7165	6957	137	4.06	4.07	0.12
8626053	14.384	F4V	6217	6024	145	4.306	4.12	0.17
8767298	14.558	F5V	6442	6500	221	4.475	4.09	0.13

(*Continued*)

Table 2. (*Continued*).

KIC number	K_p mag	LAMOST spectral type	KIC T_{eff}	LAMOST T_{eff}	LAMOST T_{eff} error	KIC log g[c]	LAMOST log g	LAMOST log g error
8773083	14.000	F6V	5931	6216	91	4.105	4.11	0.12
9238849	14.296	F5V	6056	6513	100	4.122	4.13	0.11
9479588[a]	14.723	F7IV	6141	6295	106	4.304	4.13	0.11
9479588	14.723	F5	6141	6331	103	4.304	4.14	0.12
9724292	14.397	F0III	6807	7215	157	4.07	3.8	0.14
9905069	14.582	F6IV	6498	6123	109	4.202	4.09	0.14
9905074[a]	14.570	F5V	6424	6315	122	4.454	4.15	0.13
9905074	14.570	F5	6424	6331	103	4.454	4.14	0.12

[a]Three stars have two LAMOST spectra taken months apart that give different T_{eff}/log g interpretation.
[b]Two stars are among those on our list of "constant" stars within the pulsation instability region seen in Figures 1a and 1b. The LAMOST-determined T_{eff} are significantly lower for these two stars and would place them to the red of the instability regions (Figure 5b).
[c]The KIC gives log g to three digits after the decimal, and so these digits were retained even though the log g value is not likely to be this accurate.

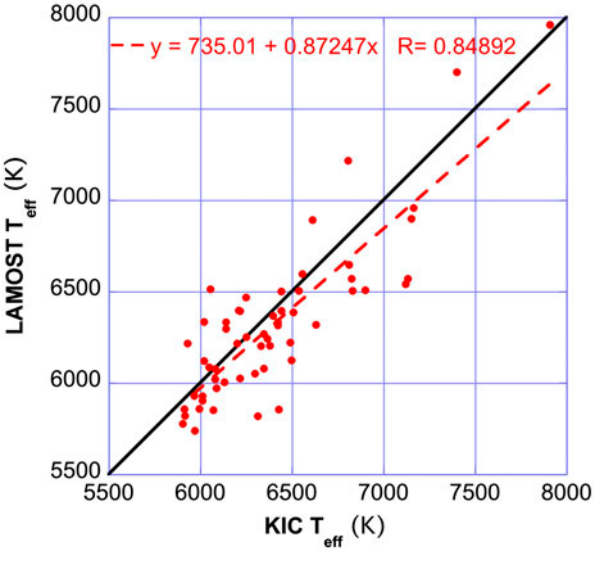

Figure 3a. LAMOST T_{eff} vs. KIC T_{eff} for 54 stars with T_{eff} derived from LAMOST spectra. Three stars have two different spectra and T_{eff} derivations. The black line (slope = 1) shows the trend if the temperatures were in agreement. The red line shows a least-squares fit to the data (slope = 0.87, correlation coefficient 0.85), indicating the spectroscopically derived T_{eff} are on average slightly lower than those of the KIC T_{eff}, opposite in sign to the average corrections found by [28] from Sloan photometry-derived T_{eff} for stars of these A–F spectral types.

As in Paper 1, we applied a 229 K increase to the effective temperature given by the KIC. This shift is used to roughly account for the systematic offset between temperatures given in the KIC and Sloan Digital Sky Survey photometry for the temperature range of our stellar sample as determined by [28,29]. To determine this shift, we averaged the five temperature offsets given in table 8 of [28] for effective temperatures 6200–6600 K. The 1-sigma error in these offsets is about 35 K.

Note that the instability strip boundaries in Figures 1a and 1b were derived from ground-based pre-*Kepler* observations of known γ Dor and δ Sct stars with relatively accurate determinations of $T_{\rm eff}$ and log g from multicolor photometry or spectroscopy. The instability region boundaries derived from theoretical stellar evolution models depend on many factors, including helium and element abundance, abundance mixtures, and convection treatment. The instability region boundaries predicted by theory were in relatively good agreement with the ground-based observations prior to the *Kepler* data; however, the distribution of the many new δ Sct and γ Dor candidates studied by KASC indicate that the instability strip boundaries may be wider than predicted by theoretical models and defined by pre-*Kepler* ground-based observations (see e.g. [19]), or that additional pulsation instability mechanisms may need to be considered to explain the data.

Figure 1a shows that 34 of the 990 "constant" stars, or only 1.6% of the entire sample, lie within the instability strip boundaries derived from the ground-based variable star observations. The uncertainties on $T_{\rm eff}$ and log g for our sample may mean that some of the stars in our sample are not in the instability regions, but just as easily, some of the stars just outside the instability region may lie within the instability region. Table 1 lists the 34 stars, along with their *Kepler* magnitude, KIC log g and KIC $T_{\rm eff}$ with and without the +229 K offset. Figure 1b shows the same diagram as in Figure 1b, except without the +229 K offset applied to the KIC $T_{\rm eff}$ values. If the offset is not applied, only 17 "constant" stars remain in the instability regions.

We show the light curves and amplitude spectra from the Fourier transforms for six of the hottest of these stars Figures 2a–2f that will lie within the pulsation instability

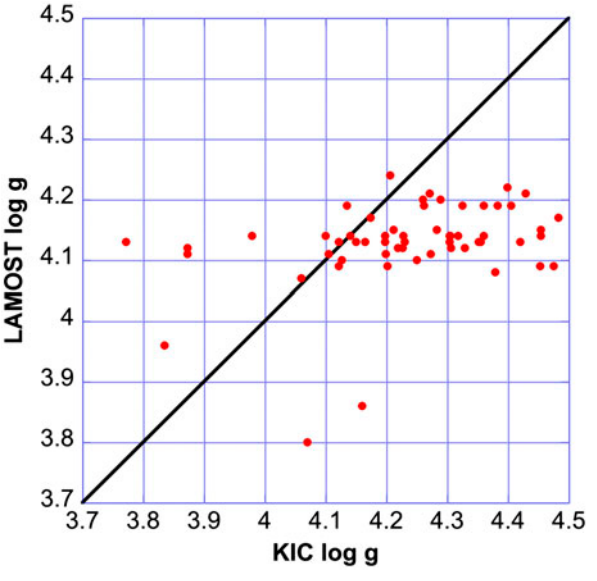

Figure 3b. LAMOST log g vs. KIC log g for 54 stars with $T_{\rm eff}$ derived from LAMOST spectra. Three stars have two different spectra and $T_{\rm eff}$ derivations. The black line shows the trend if the log g values were in agreement. The LAMOST log g values plateau at values of about 4.2 for stars of these spectral types, whereas the KIC values are spread to values as high as 4.5.

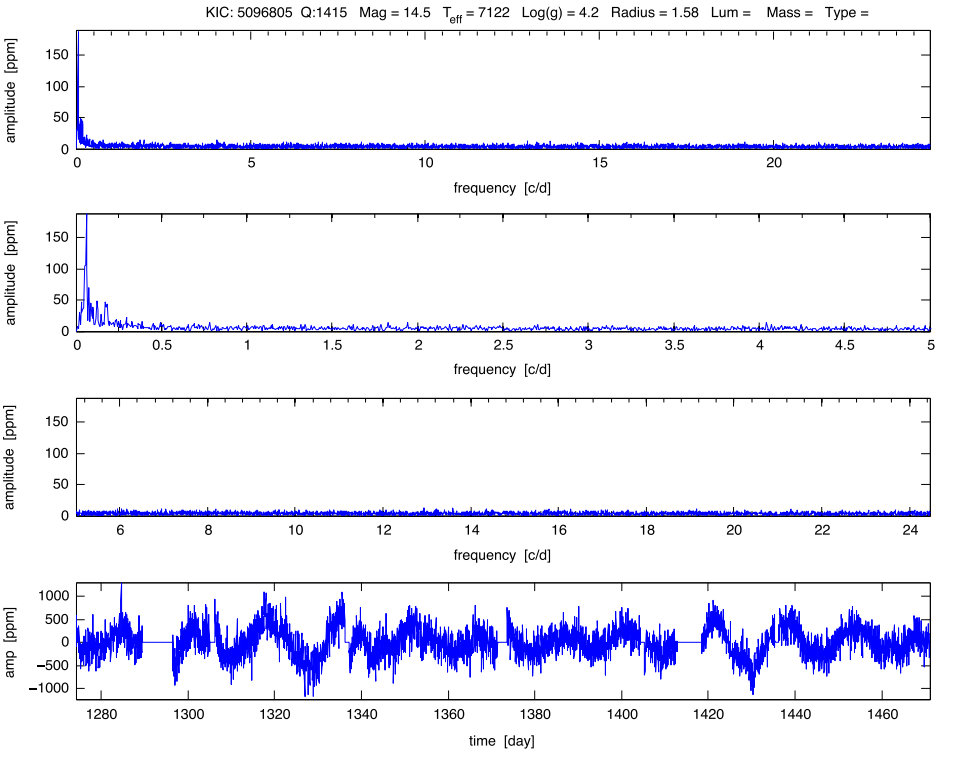

Figure 4a. KIC 5096805 light curve (bottom panel) and amplitude spectrum (top panels), categorized as a "constant" star by our amplitude spectrum criteria. The light curve variations are indicative of starspots rotating in and out of visibility and changing in size. The LAMOST-derived $T_{\rm eff}$ for this star is almost 600 K cooler than the KIC $T_{\rm eff}$ value of 7122 K, and, if adopted, would place it outside of the pulsation instability region (Figure 5b).

regions of Figures 1a and 1b whether or not the +229 K $T_{\rm eff}$ offset is applied. The figure captions include comments on the light curve and amplitude spectrum details.

5. $T_{\rm eff}$ and log g determinations from LAMOST spectra

Because our sample of *Kepler* stars is faint ($K_{\rm p}$ mag 14–16), temperatures, metallicities, and surface gravities obtained spectroscopically were not available when the targets were selected. The LAMOST (Large Sky Area Multi-Object Fiber Spectroscopic Telescope) project [30,31] is in the process of obtaining and analyzing spectra of thousands of stars in the *Kepler* field-of-view. As of this writing, 54 of our 2137 stars had been observed with LAMOST; a few had more than one spectra taken and reduced months apart. Table 2 compares the $T_{\rm eff}$ and log g derived from the LAMOST spectra with the KIC $T_{\rm eff}$ and log g values for these 54 stars. The uncertainties reflect the internal precision of the spectroscopic reduction method; the actual uncertainties may be higher.

Figures 3a and 3b show the KIC $T_{\rm eff}$ and log g plotted against the values derived from LAMOST spectra. The LAMOST $T_{\rm eff}$ values are sometimes higher, and sometimes lower than the KIC values, with the difference typically $\sim$200 K. A least-squares

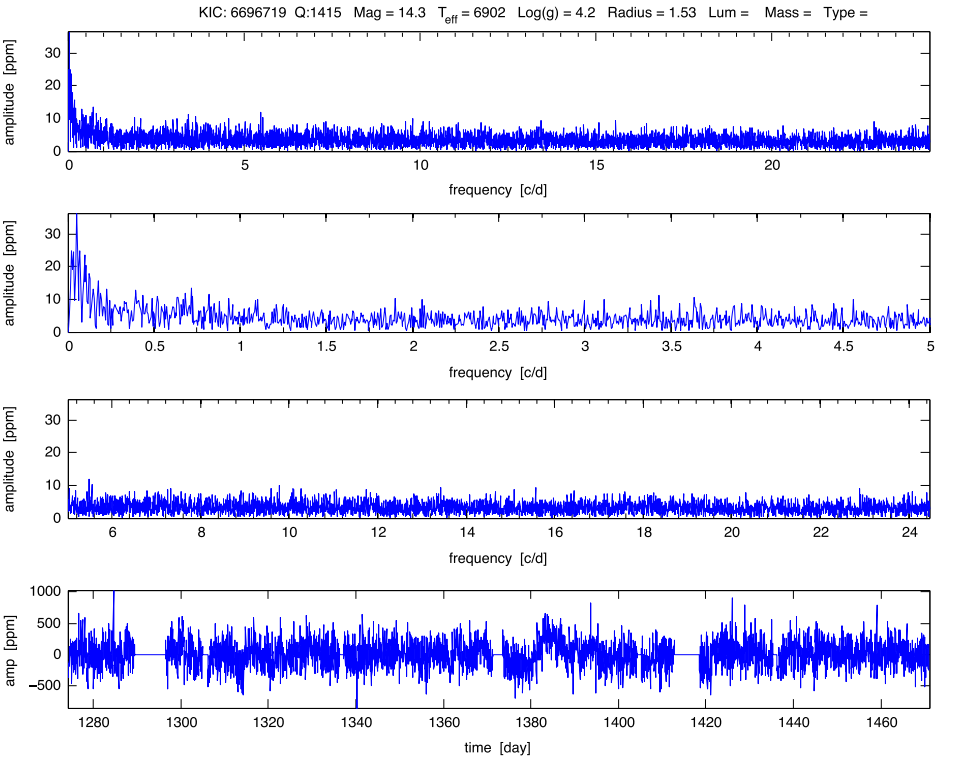

Figure 4b. KIC 6696719 light curve (bottom panel) and amplitude spectrum (top panels), categorized as a "constant" star. The LAMOST-derived $T_{\rm eff}$ for this star is almost 400 K cooler than the KIC $T_{\rm eff}$ value of 6902 K, and, if adopted, would place this star outside of the pulsation instability region (Figure 5b).

fit shows that the LAMOST-derived $T_{\rm eff}$ values tend to be slightly lower on average than the KIC values, opposite to the average difference determined by the study of [28] using SDSS color photometry. The plot of LAMOST-derived log g vs. KIC log g shows that the log g reaches a plateau at about 4.2, whereas the KIC log g continues to increase to 4.5. An average overestimation bias of about 0.23 dex in KIC log g was noted by [32].

In Table 2 are highlighted the two "constant" stars near the red edge of the pulsation instability regions that also have LAMOST-derived $T_{\rm eff}$ and log g. Figures 4a and 4b show the light curves and amplitude spectra of these stars. The LAMOST $T_{\rm eff}$ is 582 K lower for KIC 5096805, and 395 K lower for KIC 6696719. Figures 5a and 5b show a zoom-in on the pulsation instability regions with and without the +229 K $T_{\rm eff}$ offset. Both of these stars would move to the red of the instability regions if the LAMOST-derived $T_{\rm eff}$ were to be adopted (see arrows in Figure 5b).

It is possible that the spectroscopically derived $T_{\rm eff}$ for other "constant" stars would also be lower, moving them out of the pulsation instability regions. However, for some of the "constant" stars in the center or toward the blue of the δ Sct instability regions, $T_{\rm eff}$ changes to the KIC values greater than the average errors would be required to move them entirely out of the instability regions. Figures 6a and 6b show the "constant" star sample of Figure 1b (without the +229 K offset), and with the sample

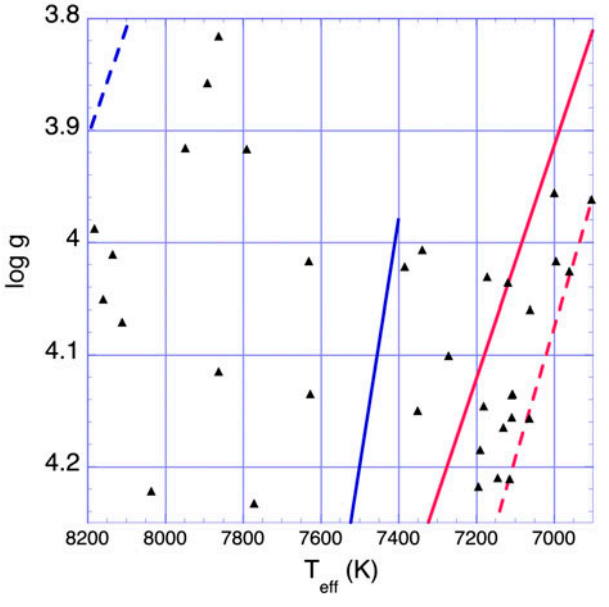

Figure 5a. Enlargement of pulsation instability region of Figure 1a including the +229 K offset from KIC $T_{\rm eff}$ values. The 34 "constant" stars of Table 1 are shown here. The symbols for two stars with nearly the same $T_{\rm eff}$ and log g (KIC 7364349 and KIC 8292900) overlap.

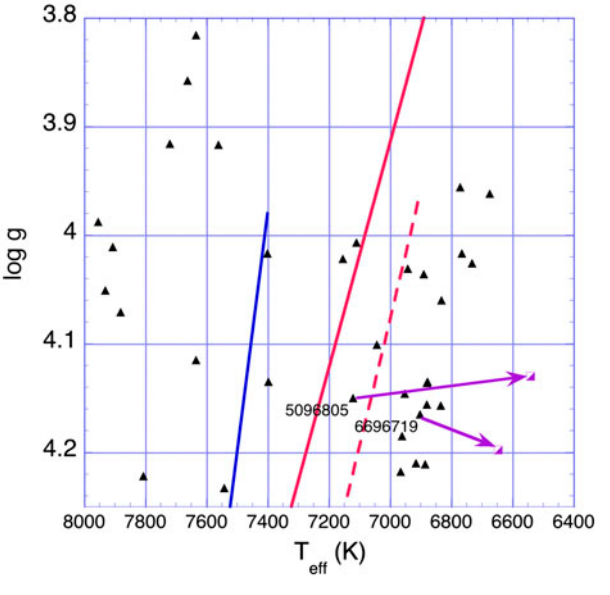

Figure 5b. Same as Figure 5a, but without the +229 K offset applied to the KIC $T_{\rm eff}$, and with two stars labeled that have $T_{\rm eff}$ and log g determined by LAMOST spectra. These stars would lie to the red of instability regions by several hundred K (purple arrows) if the LAMOST $T_{\rm eff}$ were used instead of the KIC $T_{\rm eff}$ value.

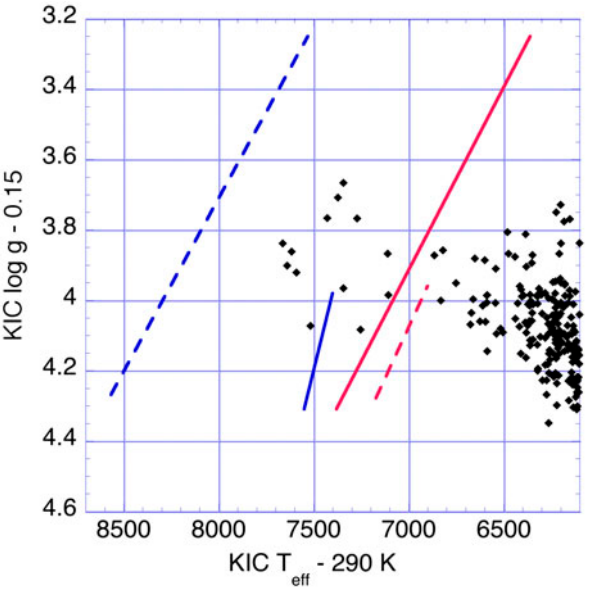

Figure 6a. Same as Figure 1b, but with −290 K and −0.15 dex applied to KIC $T_{\rm eff}$ and log g. In this plot, 15 stars lie within the pre-*Kepler* pulsation instability regions.

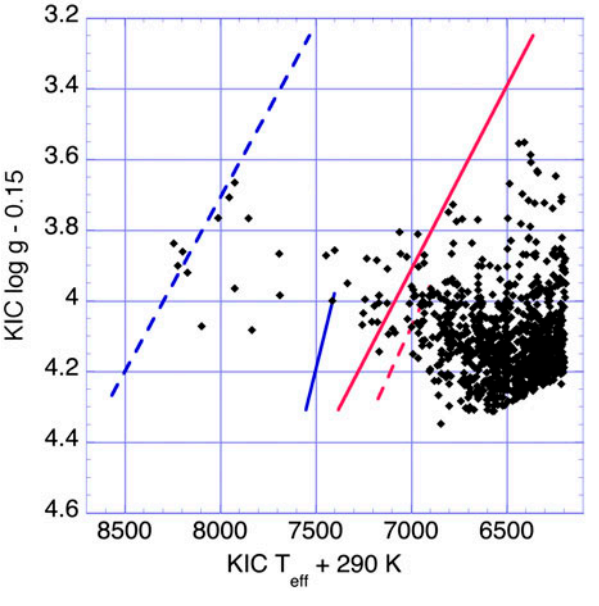

Figure 6b. Same as Figure 1b, but with +290 K and −0.15 dex applied to KIC $T_{\rm eff}$ and log g. In this plot, 52 stars lie within the pre-*Kepler* pulsation instability regions.

stars moved by an average (random) $T_{\rm eff}$ error of ± 290 K taken from [19]. We also moved all of the stars in log g by −0.15 dex to roughly take into account the

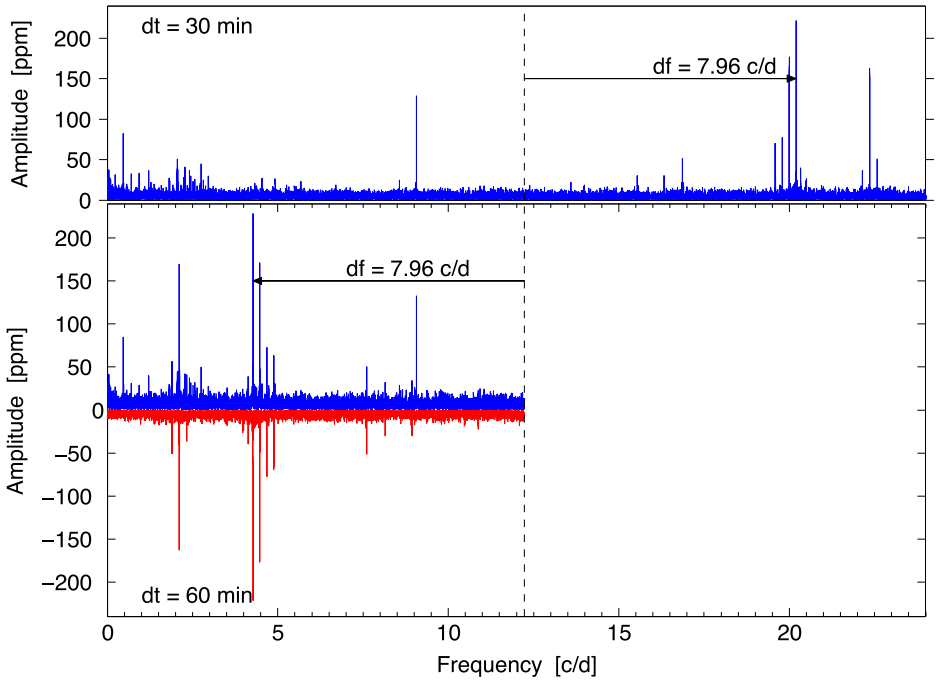

Figure 7. Top panel: Amplitude spectrum from Fourier transform of light curve for *Kepler* B star taken in long cadence, with Nyquist frequency 24.4 c/d. Bottom panel: Amplitude spectrum from Fourier transform of same light curve sub-sampled at 1-h cadence, with Nyquist frequency 12.2 c/d. The super-Nyquist frequencies seen on the top panel are "mirrored" at low frequency. The amplitude spectrum above 12.2 c/d from the top panel is inverted and reflected (red) to compare with the spectrum in the sub-sampled light curve.

systematically higher average log g in the KIC catalog values vs. the LAMOST log g for log $g > 4.2$, and the KIC overestimation bias found by [32]. In the first case (Figure 6a), 15 sample stars remain within the ground-based pre-*Kepler* pulsation instability regions, and in the second case (Figure 6b), 52 stars remain. Therefore it is likely that, if the KIC $T_{\rm eff}$ errors are random, at least some "constant" stars that should show pulsations remain to be explained.

6. Super-Nyquist frequencies

Among the list of explanations for the "constant" stars given in Paper 1 is the possibility that the "constant" stars are pulsating at frequencies higher than the 24.4 c/d Nyquist frequency for long-cadence *Kepler* data. However, [22] show that super-Nyquist frequencies do appear in Fourier transforms of the long-cadence data at a lower frequency reflected below the Nyquist frequency. If the data-set is long enough (of order 1 year), the Nyquist reflections may even be distinguishable from real frequencies via their side-lobes, and therefore the true super-Nyquist frequency may be determined.

To illustrate this effect, we show in Figure 7 the amplitude spectrum for a *Kepler* B star observed in long cadence ($\sim$30 min integration per data point, top panel), with Nyquist frequency 24.4 c/d. Some high-frequency peaks are evident at about 20 c/d.

The bottom panel shows the amplitude spectrum obtained using the light curve sampled every $\sim$1 h, so the Nyquist frequency is 12.2 c/d (vertical dashed line). The frequencies above the 24.4 c/d Nyquist frequency from the first panel can be seen "mirrored" below the 12.2 c/d Nyquist frequency. The arrow highlights the highest amplitude peak at 7.96 c/d above the Nyquist frequency that shows up at 7.96 c/d below the Nyquist frequency for the sub-sampled set. The red curve shows the amplitude spectrum above 12.2 c/d from the top panel inverted and reflected to compare with the spectrum in the sub-sampled light curve.

We conclude that it is unlikely that any of our "constant" stars have pulsation frequencies above the Nyquist frequency 24.4 c/d at amplitudes typical of γ Dor or δ Sct pulsations (>100 ppm), as their reflections should appear at lower frequencies in the Fourier transform. If this were the case, a time series of at least a year of long-cadence data would be needed to distinguish a Nyquist reflection frequency from a true frequency, as the barycentric time corrections to the *Kepler* data then begin to create detectable sidelobe peaks around the super-Nyquist frequency peaks.[22]

7. Remaining explanations for "constant" stars

While we have discussed two of the five explanations suggested for the "constant" stars in Paper 1, we have not addressed three others. First, the stars may be pulsating in higher spherical harmonic degree modes (e.g. degree >0–3) that are not easily detectable photometrically. Such high-degree modes may be detectable spectroscopically, but high resolution and time series spectra for such faint stars require continuous observation for weeks with 10-m class telescopes, and are impossible to organize. It is interesting that for a few brighter γ Dor stars where multisite spectroscopic data have been collected and analyzed, frequencies first detected photometrically are also seen spectroscopically via their line-profile variations [33, e.g. HD 12901,], while for other γ Dor stars, there seems to be almost no relationship between frequencies detected spectroscopically, and those found photometrically [34, 35], e.g. HD 49434,].

Second, as can be seen from some of the example constant-star power spectra in Figures 2a–2f, there may be pulsation modes with amplitudes at or below the noise level of this data; the modes could possibly be detected with a longer time series or by reducing the noise levels, possibly making use of the *Kepler* pixel data. Third, a physical mechanism may be operating, e.g. diffusive helium or element settling, which inhibits pulsations for some stars.

Murphy et al. [36] identified about 50 bright (V magnitude $\leq$ 10), non-chemically peculiar stars in or near the δ Sct instability region observed by *Kepler* that showed no variability at δ Sct p-mode frequencies of 5–50 c/d with amplitude higher than 50 μmag. They used high-resolution spectroscopic observations to derive a more accurate $T_{\rm eff}$ and log g, as well as $v \sin i$ and metallicity. They find that many of their non-pulsating stars could plausibly lie outside the δ Sct instability region due to remaining uncertainties in $T_{\rm eff}$ or if the star was actually a binary and misinterpreted as a single star. However, they find one non-pulsating chemically normal star in the center of the δ Sct pulsation region that remains to be explained.

8. Distribution of "non-constant" stars

Figures 8a and 8b show how the remaining 1147 "non-constant" stars are distributed in relation to the instability regions established from ground-based observations, with and

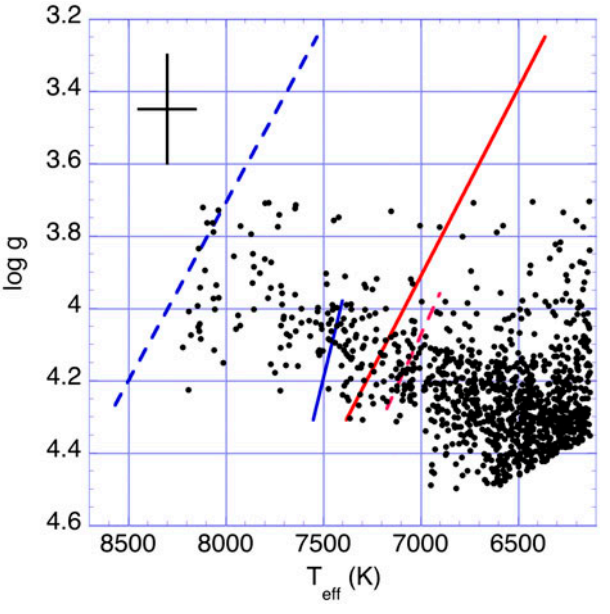

Figure 8a. Location of 1147 sample stars that are not "constant" (see definition in text) in the log g–$T_{\rm eff}$ diagram, along with the δ Sct (dashed lines) and γ Dor (solid lines) instability strip boundaries established from pre-*Kepler* ground-based observations.[26,27] The $T_{\rm eff}$ of the stars has been shifted by +229 K to account for the systematic offset in temperatures of the *Kepler* Input Catalog and SDSS photometry for this temperature range as determined by [28]. The black cross shows an error bar on log g (0.3 dex) and $T_{\rm eff}$ (290 K) determined by comparisons of KIC values and values derived from ground-based spectroscopy for brighter *Kepler* targets.[19] Most of these stars have light curves consistent with stellar activity (spots) or binarity.

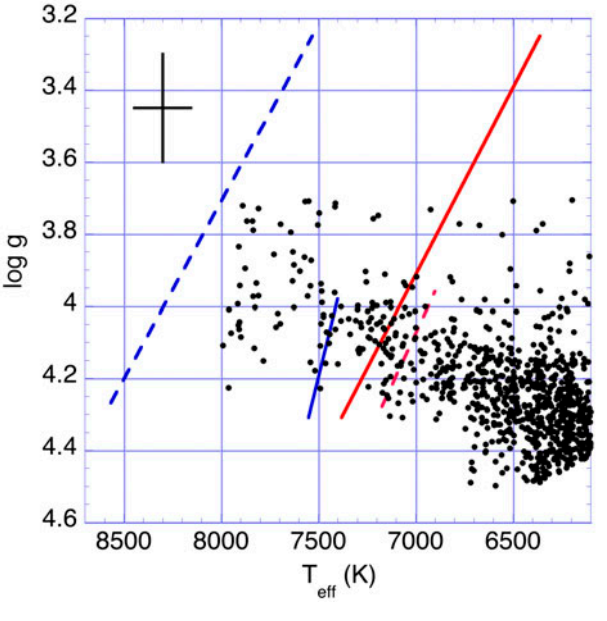

Figure 8b. Same as Figure 8a without the +229 K offset applied to the KIC $T_{\rm eff}$.

without the +229 K offset applied to the KIC $T_{\rm eff}$. [3, 4] discuss and categorize the "non-constant" stars in the combined set of stars observed in Q6–13 and Q14–17. The light curves of many of these stars show irregular low-frequency variations consistent with rotating spots or stellar activity; many are eclipsing binaries. [37–40] and [20] discuss the light-curve properties of many of the A–F stars observed by *Kepler*. As discussed by [3, 4] and as also found by [19] and [18], δ Sct and γ Dor candidates lie outside the pulsation instability regions established by ground-based observations. Additional pulsation driving mechanisms may be needed to explain the observed frequencies. A new pulsation mechanism involving fluctuations in turbulent pressure in the hydrogen-ionization region, for example, has been proposed to explain pulsations at δ Sct-like frequencies by [41].

9. Conclusions and future work

In Paper I discussing a sample of 633 A–F main-sequence stars observed by *Kepler* during Quarters 6–13, 359 stars, or roughly 60%, were found to be "constant", defined as showing no frequencies above 20 ppm in their light curves between 0.2 and 24.4 c/d. In that sample, we found very few (only six) photometrically non-varying stars within the γ Dor and δ Sct pulsation instability regions established by pre-*Kepler* ground-based observations. Here, in our sample of 2137 stars observed by *Kepler* in Quarters 14–17, 990 stars, or 46% were found to be "constant", with 34 of these stars lying within the pulsation instability regions. The percentage of "constant" stars is lower because the targets were selected by cross-correlating with the list of stars that showed variability in Q0 full-frame images.

We compare the KIC $T_{\rm eff}$ with the $T_{\rm eff}$ derived for 54 stars in common with our GO targets with $T_{\rm eff}$ derived from LAMOST spectroscopy. While there is significant scatter, on average the LAMOST-derived $T_{\rm eff}$ is the same or slightly smaller than the KIC $T_{\rm eff}$; therefore, it is questionable whether we should have applied a +229 K increase to the KIC $T_{\rm eff}$ for stars of this spectral type, as suggested by the analysis of [28] using Sloan multicolor photometry. Without the offset, only 17 stars lie within the instability region. For two "constant" stars with LAMOST observations, adopting the LAMOST-derived $T_{\rm eff}$ moves them to the red of the instability regions. A likely explanation for many of the "constant" stars within the instability region is therefore that their KIC $T_{\rm eff}$ and/or log g is not correct. However, for some of the hottest constant stars, the $T_{\rm eff}$ adjustment from KIC would be quite large; in addition, $T_{\rm eff}$ or log g adjustments may also move some "constant" stars that are outside of the instability regions into the instability regions, so there may be many "constant" stars that should be pulsating that remain to be explained.

It is also unlikely that "constant" stars actually have undetected frequencies above the long-cadence Nyquist frequency. As [22] show, and as we also illustrate, such frequencies would be mirrored below the Nyquist frequency and be visible unless the amplitudes are low compared to the noise level.

For future work, we hope to make use of LAMOST data to improve $T_{\rm eff}$, log g, and metallicity determinations for these faint stars, and model some of the "constant" stars that may still lie within the instability regions. We also could use the *Kepler* pixel data or refined light curve analyses to reduce noise levels to establish the significance of modes with very low amplitudes. We would like to use stellar modeling to determine how much diffusive settling is possible and necessary to eliminate pulsations in γ Dor or δ Sct stars. We also hope to carry out model calculations to explore alternate

pulsation driving mechanisms that may help explain the *Kepler* stars that show pulsations at unexpected frequencies or lie outside of predicted instability boundaries.

Acknowledgements

The authors are grateful for data and funding through the NASA *Kepler* Guest Observer Program Cycles 1-4. KU acknowledges financial support by the Spanish National Plan of R&D for 2010, project AYA2010-17803. This work has benefited from funding by the Project FP7-PEOPLE-IRSES: ASK no 269194. J.G. thanks S. Murphy and H. Shibahashi for useful discussions.

Disclosure statement

No potential conflict of interest was reported by the authors.

References

[1] Borucki, WJ, Koch D, Basri G, Batalha N, Brown T, Caldwell D, Caldwell J, Christensen-Dalsgaard J, Cochran WD, DeVore E, Dunham EW, Dupree AK, Gautier TN, Geary JC, Gilliland R, Gould A, Howell SB, Jenkins JM, Kondo Y, Latham DW, Marcy GW, Meibom S, Kjeldsen H, Lissauer JJ, Monet DG, Morrison D, Sasselov D, Tarter J, Boss A, Brownlee D, Owen T, Buzasi D, Charbonneau D, Doyle L, Fortney J, Ford EB, Holman MJ, Seager S, Steffen JH, Welsh WF, Rowe J, Anderson H, Buchhave L, Ciardi D, Walkowicz L, Sherry W, Horch E, Isaacson H, Everett ME, Fischer D, Torres G, Johnson JA, Endl M, MacQueen P, Bryson ST, Dotson J, Haas M, Kolodziejczak J, Van C, Jeffrey C, Hema T, Joseph D, Quintana EV, Clarke BD, Allen C, Li J, Wu H, Tenenbaum P, Verner E, Bruhweiler F, Barnes J, Prsa A. *Kepler* planet-detection mission: Introduction and first results. Science. 2010;327:977–980.

[2] Gilliland RL, Brown TM, Christensen-Dalsgaard J, Kjeldsen H, Aerts C, Appourchaux T, Basu S, Bedding TR, Chaplin WJ, Cunha MS, De CP, De Ridder J, Guzik JA, Handler G, Kawaler S, Kiss L, Kolenberg K, Kurtz DW, Metcalfe TS, Monteiro MJPFG, Szabó R, Arentoft T, Balona L, Debosscher J, Elsworth YP, Quirion P-O, Stello D, Suárez JC, Borucki WJ, Jenkins JM, Koch D, Kondo Y, Latham DW, Rowe JF, Steffen JH. *Kepler* asteroseismology program: introduction and first results. Publ. Astron. Soc. Pacific. 2010;122:131–143.

[3] Bradley PA, Guzik JA, Miles LF, Jackiewicz J, Uytterhoeven K, Kinemuchi K. Analysis of γ Doradus and δ Scuti stars observed by *Kepler*. In: Guzik JA, Chaplin W, Handler G, Pigulski A, editors. Precision asteroseismology, IAU symposium 301; 2013 August; Wroclaw, Poland; 2014. p. 387–388.

[4] Bradley PA, Guzik JA, Miles LF, Jackiewicz J, Uytterhoeven K, Kinemuchi K. Results of a search for γ Doradus and δ Scuti stars with the *Kepler* spacecraft. Astron. J. 2015;149:68–81.

[5] Gaulme P, Guzik JA. Searching for pulsations in *Kepler* eclipsing binary stars. In: Guzik JA, Chaplin W, Handler G, Pigulski A, editors. Precision asteroseismology, IAU symposium 301; 2013 August; Wroclaw, Poland; 2014. p. 413–414.

[6] Guzik JA, Bradley PA, Jackiewicz J, Uytterhoeven K, Kinemuchi K. The occurrence of non-pulsating stars in the γ Doradus/δ Scuti pulsation instability region. Astron. Rev. 2013;8.4:4–30; arXiv:1403.8013 (Paper 1, 2013).

[7] Guzik JA, Bradley PA, Jackiewicz J, Uytterhoeven K, Kinemuchi K. The occurrence of non-pulsating stars in the γ Doradus and δ Scuti pulsation instability regions. In: Guzik JA, Chaplin W, Handler G, Pigulski A, editors. Precision asteroseismology, IAU symposium 301; 2013 August; Wroclaw, Poland; 2014. p. 63–66.

[8] Balona LA, Krisciunas K, Cousins AWJ. γ Doradus: evidence for a new class of pulsating star. Monthly Not. Roy. Astron. Soc. 1994;270:905–913.

[9] Kaye AB, Handler G, Krisciunas K, Poretti E, Zerbi FM. γ Doradus stars: defining a new class of pulsating variables. Publ. Astron. Soc. Pacific. 1999;111:840–844.

[10] Henry G, Fekel FC, Henry SM. Photometry and spectroscopy of 11 γ Doradus stars. Astron. J. 2007;133:1421–1440.
[11] Guzik JA, Kaye AB, Bradley PA, Cox AN, Neuforge C. Driving the gravity-mode pulsations in γ Doradus variables. Astrophys. J. Lett. 2000;542:L57–L60.
[12] Dupret MA, Grigahcéne A, Garrido R, Gabriel M, Scuflaire R. Theoretical instability strips for δ Scuti and γ Doradus stars. Astron. Astrophys. 2004;414:L17–L20.
[13] Dupret M-A, Grigahcène A, Garrido R, Gabriel M, Scuflaire R. Convection-pulsation coupling. II. Excitation and stabilization mechanisms in δ Sct and γ Dor stars. Astron. Astrophys. 2005;435:927–929.
[14] Grigahcéne A, Dupret M-A, Garrido R, Gabriel M. Influence of overshooting and metallicity on the δ Scuti and γ Doradus instability strips. Mem. Sa. Astron. Italiana. 2006;7:129–130.
[15] Rodriguez E, López-González MJ, López de Coca P. A revised catalog of δ Scuti stars. Astron. Astrophys. Suppl. Ser. 2000;144:469–474.
[16] Chevalier C. Short-period variables. VIII. Evolution and pulsation of δ Scuti stars. Astron. Astrophys. 1971;14:24–31.
[17] Turcotte S, Richer J, Michaud G. Consistent evolution of F stars: diffusion, radiative accelerations, and abundance anomalies. Astrophys. J. 1998;504:559–572.
[18] Grigahcène A, Antoci V, Balona L, Catanzaro G, Daszyńska-Daszkiewicz J, Guzik JA, Handler G, Houdek G, Kurtz DW, Marconi M, Monteiro, MJPFG, Moya A, Ripepi V, Suárez J-C, Uytterhoeven K, Borucki, WJ, Brown TM, Christensen-Dalsgaard J, Gilliland RL, Jenkins JM, Kjeldsen H, Koch D, Bernabei S, Bradley P, Breger M, Di Criscienzo M, Dupret M-A, García RA, García Hernández A, Jackiewicz J, Kaiser A, Lehmann H, Martín-Ruiz S, Mathias P, Molenda-Żakowicz J, Nemec JM, Nuspl J, Paparó M, Roth M, Szabó R, Suran MD, Ventura R. Hybrid γ Doradus-δ Scuti pulsators: new Insights into the physics of the oscillations from *Kepler* observations. Astrophys. Lett. 2010;713L:192–L197.
[19] Uytterhoeven K, Moya A, Grigahcène A, Guzik JA, Gutiérrez-Soto J, Smalley B, Handler G, Balona LA, Niemczura E, Fox ML, Benatti S, Chapellier E, Tkachenko A, Szabó R, Suárez JC, Ripepi V, Pascual J, Mathias P, Martín-Ruíz S, Lehmann H, Jackiewicz J, Hekker S, Gruberbauer M, García RA, Dumusque X, Díaz-Fraile D, Bradley P, Antoci V, Roth M, Leroy B, Murphy SJ, De Cat P, Cuypers J, Kjeldsen H, Christensen-Dalsgaard J, Breger M, Pigulski A, Kiss LL, Still M, Thompson SE, van Cleve J. The *Kepler* characterization of the variability among A- and F-type stars. Astron. Astrophys. 2011;534 Article ID A125, 70 p.
[20] Balona LA, Dziembowski W. *Kepler* observations of δ Scuti stars. Monthly Not. Roy. Astron. Soc. 2011;417:591–601.
[21] Jenkins JM, Caldwell DA, Chandrasekaran H, Twicken JD, Bryson ST, Quintana EV, Clarke BD, Li J, Allen C, Tenenbaum P, Wu H, Klaus TC, Middour CK, Cote MT, McCauliff S, Girouard FR, Gunter JP, Wohler B, Sommers J, Hall JR, Uddin AKMK, Wu MS, Bhavsar PA, Van Cleve J, Pletcher DL, Dotson JA, Haas MR, Gilliland RL, Koch DG, Borucki WJ. Overview of the *Kepler* science processing pipeline. Astrophys. J. Lett. 2010;713L:87–L91.
[22] Murphy SJ, Shibahashi H, Kurtz DW. SuperNyquist asteroseismology with the *Kepler* space telescope. Monthly Not. Roy. Astron. Soc. 2013;430:2896–2988.
[23] Latham DW, Brown TM, Monet DG, Everett M, Esquerdo GA, Hergenrother CW. The *Kepler* input catalog. Bull. Am. Astron. Soc. Meeting 207. 2005;37:1340.
[24] Kinemuchi K, Still M, Fanelli M. Kepler Science Team. *Kepler* full-frame image variable star catalog. Bull. Am. Astron. Soc. 2011;43:21720106.
[25] McNamara B, Jackiewicz J, McKeever J. The classification of *Kepler* B-star variables. Astron. J. 2012;143:101–112.
[26] Rodriguez E, Breger M. δ Scuti and related stars: analysis of the R00 catalogue. Astron. Astrophys. 2001;366:178–196.
[27] Handler G, Shobbrook RR. On the relationship between the δ Scuti and γ Doradus pulsators. Monthly Not. Roy. Astron. Soc. 2002;333:251–262.
[28] Pinsonneault MH, An D, Molenda-Zakowicz J, Chaplin WJ, Metcalfe TS, Bruntt H. A revised effective temperature scale for the *Kepler* Input Catalog. Astrophys. J. Suppl. Ser. 2012;199:Article ID 30, 22 p.

[29] Pinsonneault MH, An D, Molenda-Zakowicz J, Chaplin WJ, Metcalfe TS, Bruntt H. Erratum: a revised effective temperature scale for the *Kepler* input catalog. Astrophys. J. Suppl. Ser. 2013;208:Article ID 12, 5 p.
[30] Molenda-Żakowicz J, Sousa, SG, Frasca A, Uytterhoeven K, Briquet M, Van Winckel H, Drobek D, Niemczura E, Lampens P, Lykke J, Bloemen S, Gameiro JF, Jean C, Volpi D, Gorlova N, Mortier A, Tsantaki M, Raskin G. Atmospheric parameters of 169 F-, G-, K- and M-type stars in the *Kepler* field. Monthly Not. Roy. Astron. Soc. 2013;434:1422–1434.
[31] Molenda-Zakowicz J, De Cat P, Fu J.-N., Yang X.-H. and the LAMOST- *Kepler* collaboration. LAMOST observations in the *Kepler* field. In: Guzik JA, Chaplin WJ, Handler G, Pigulski A, editors. Precision asteroseismology, IAU symposium 301, August 2013. Wroclaw, Poland; 2014. p. 457–458.
[32] Verner GA, Chaplin WJ, Basu S, Brown TM, Hekker S, Huber D, Karoff C, Mathur S, Metcalfe TS, Mosser B, Quirion P-O, Appourchaux T, Bedding TR, Bruntt H, Campante TL, Elsworth Y, García RA, Handberg R, Régulo C, Roxburgh IW, Stello D, Christensen-Dalsgaard J, Gilliland RL, Kawaler SD, Kjeldsen H, Allen C, Clarke BD, Girouard FR. Verification of the *Kepler* input catalog from asteroseismology of solar-type stars. Astrophys. J. Lett. 2011;738:L28, 5 p.
[33] Brunsden E, Pollard KR, Cottrell PL, Wright DJ, De Cat P. Spectroscopic pulsational frequency identification and mode determination of γ Doradus star HD 12901. Monthly Not. Roy. Astron. Soc. 2012;427:2512–2522.
[34] Brunsden E, Pollard KR, Cottrell PL, Wright DJ, De Cat P, Kilmartin PM. Spectroscopy of γ Dor stars. In: Guzik JA, Chaplin WJ, Handler G, Pigulski A, editors. Precision asteroseismology, IAU symposium 301; 2013 August; Wroclaw, Poland; 2014. p. 113–116.
[35] Brunsden E, Pollard KR, Cottrell PL, Uytterhoeven K, Wright DJ, De Cat P. The classification of frequencies in the γ Doradus / δ Scuti hybrid star HD 49434. Monthly Not. Roy. Astron. Soc. 2015;447:2970–2980.
[36] Murphy S, Bedding TJ, Niemszura E, Kurtz DW, Smalley B. A search for non-pulsating, chemically normal stars in the δ Scuti instability strip using *Kepler* data. Monthly Not. Roy. Astron. Soc., 2015;447:3948–3959.
[37] Balona LA. Rotational light variations in *Kepler* observations of A-type stars. Monthly Not. Roy. Astron. Soc. 2011;415:1691–1702.
[38] Balona LA. Activity in A-type stars. Monthly Not. Roy. Astron. Soc. 2013;431:2240–2252.
[39] Balona LA. Low frequencies in *Kepler* δ Scuti stars. Monthly Not. Roy. Astron. Soc. 2014;437:1476–1484.
[40] Balona LA, Guzik JA, Uytterhoeven K, Smith JC, Tenenbaum P, Twicken JD. The *Kepler* view of γ Doradus stars. Monthly Not. Roy. Astron. Soc. 2011;415:3531–3538.
[41] Antoci V, Cunha M, Houdek G, Kjeldsen H, Trampedach R, Handler G, Lüftinger T, Arentoft T, Murphy S. The role of turbulent pressure as a coherent pulsational driving mechanism: the case of the δ Scuti star HD 187547. Atrophys. J. 2014;796:Article ID 118, 8 p.